Defence Science Journal, Vol. 61, No. 1, January 2011, pp. 3-11

Published Online: 31 December 2010

Numerical Exploration of Staged Transverse Injection into Confined Supersonic Flow behind a Backward-facing Step

A.T. Sriram and Debasis Chakraborty*

Defence Research & Development Laboratory, P.O. Kanchanbagh, Hyderabad
**Email: debasis_cfd@drdl.drdo.in*

ABSTRACT

Staged transverse sonic injection into supersonic flow in a confined environment usually employed in scramjet combustor has been explored numerically using an indigenously developed three-dimensional Reynolds Averaged Navier Stokes solver with Roe's scheme and k-ω turbulence model. Simulations were carried out for both without injection and with injection in Mach 2 flow behind a backward-facing step in a rectangular duct. Simulation captured all finer details of flow structures including recirculation bubble behind a backward-facing step, barrel shocks and Mach discs caused due to transverse injection and reattachment of shear layer in the downstream wake region. K-ω turbulence model with compressibility correction performed extremely well in predicting the overall behaviour of the flow field. The jet from the second injector was found to penetrate more in the free-stream due to the loss of free-stream total pressure across the barrel shock of the first injection point. Excellent agreement of computed profiles of various flow parameters at different axial locations in the duct with experimental results and other numerical results available in the literature demonstrate the robustness and accuracy of the indigenously developed code.

Keywords: Supersonic flow, scramjet combustor, staged transverse injection

NOMENCLATURE

C_v	Specific heat at constant volume
D	Injector Diameter
E	Total energy
e	Internal energy
F,G,H	Flux vector
H,L, W	Test section height, length, width
h	Step height
k	Turbulent kinetic energy
M	Mach number
Pr	Prandtl number
p	Pressure
T	Temperature
t	Time
S	Source term
R	Residue
$\hat{R}$	Matrix of right Eigen vectors
U	State vector
u,v,w	Cartesian velocities in x,y,z directions
x,y,z	Co-ordinate diections

Greek symbols

$\alpha,\alpha^*,\beta,\beta^*\sigma,\sigma^*$	Turbulence closure coefficient
Σ	Velocity Divergence
Φ	Strain invariant
ε	Turbulent dissipation
γ	Specific heat ratio
ρ	Density
ω	Specific dissipation rate
μ	Viscosity
λ	Eigen vector
$\Delta\upsilon$	Wave length

Subscripts

L,R	Left and right state
∞	Represents a free-stream quantity
t	Turbulent property
m	Molecular property

1. INTRODUCTION

Development of airbreathing hypersonic technology has been the subject of renewed interest since the 1980's because of tremendous military and commercial opportunities. The success of efficient design of such a transatmospheric hypersonic vehicle depends largely on the proper choice of the propulsion system which is capable of producing large thrust to overcome the drag experienced by the vehicle. This type of vehicle according to current proposals, use supersonic combustion ramjet (scramjet) propulsion system. Due to supersonic flow-speed in the combustion chamber, problems arise in the mixing of reactants, flame anchoring, stability and completion of combustion within the limited combustion chamber length. Rectangular scramjet combustor with one-sided divergence is generally used for drag reduction and efficient engine-airframe integration in hypersonic

Recieved 10 December 2009, Revised 4 October 2010

airbreathing vehicles. Backward-facing step[1,2] was employed in the scramjet combustor to stabilize the flame and generate self-excited resonance. Hence, a combustor with a transverse injection downstream of a backward-facing step is one of the simplest designs to enhance mixing and flame stabilisation in a scramjet combustor.

Transverse injection into supersonic flow past a backward-facing step in a confined environment is quite complex. The schematic of flow field is shown in Fig.1. The supersonic stream expands at the base corner. The incoming turbulent boundary layer separates and forms a free shear layer that eventually reattaches and undergoes recompression. Between the separation of boundary layer at base corner and

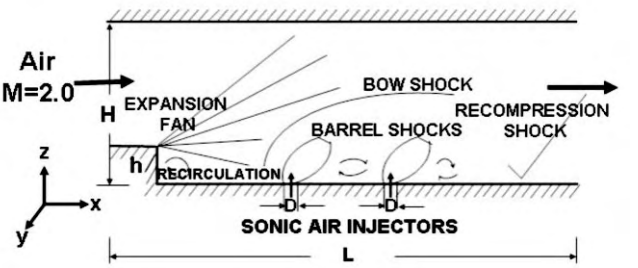

Figure 1. Schematic Representation of flow features of transverse sonic injection in three-dimensional duct.

reattachment point, there exists a low-speed recirculating flow region which is used for fuel injection and flame stabilisation. The transverse injection blocks the supersonic free-stream flow and a strong bow shock wave is formed in front of the injection point followed by a barrel shock. Downstream of the injection point, the boundary layer reattaches and a recompression shock wave is generated. Subsequent injections in the downstream of first injection causes more fuel penetration due to the loss of total pressure of the free-stream through the bow shock caused due to the first injection.

Early investigations of the transverse gaseous jet in supersonic cross flow were focused on qualitative examinations of underexpanded injection flow field and correlations were developed for injectant penetration depth as a function of various flow parameters[3,4]. Papamoschou[5], *et al.* investigated the effect of free-stream Mach number, jet Mach number, static pressure ratio, density ratio, and momentum ratio on penetration using Schlieren photography. Results indicated that jet penetration into a supersonic cross flow was principally dependent on the momentum ratio of the two streams. Penetration of the perpendicular jets behind the steps in the supersonic flow was investigated experimentally by Yamauchi[6], *et al.* to understand the effects of the merging of the recirculation bubbles at the step base and ahead of the jets. It was observed that the slope of the Mach disc height plotted versus the dynamic pressure ratio was reduced as the merger occured and the merging improved the lateral spread of the injectant near the injector and thus improved the ignition characteristics.

Kuratani[7], *et al.* and Ikeda[8], *et al.* experimentally investigated the mixing characteristics of normal injection into supersonic flow behind backward-facing step. Average and RMS velocity profiles and vorticity distribution in the compressible mixing layer between the normal injected flow and the inlet air flow were measured using PIV technique to find out the behavior of the recirculation zone and the height of the Mach discs. Although, these studies have explained important flow features of normal injection behind backward-facing step, the test section height was kept sufficiently high and the effect of confinement on the flow structure was not studied. In the practical scramjet combustor, for volume-limited application, the height of the combustor is sufficiently low and the confinement plays an important effect in the flow development.

Cold flow mixing of transverse sonic jets in a supersonic flow in a confined environment was studied experimentally by McDaniel[9,10], *et al*. Injection of two sonic transverse jets behind a backward-facing step in a Mach 2 stream was considered in a rectangular cross section. Detailed flow visualisation and extensive measurements of various flow parameters at different cross sections presented in the study is very useful to validate any CFD software. To study the evolution of supersonic mixing in the combustor, Abbitt[11], *et al*. carried out detailed measurement of mole fraction of this experimental condition.

Transverse sonic jet injections from flat plate into supersonic cross flow has been subjected to extensive numerical simulation in the recent literature[12-18]. Both two-dimensional[12-14] and three-dimensional[15-18] Navier Stokes simulations were reported. Most of the early calculations[15,16] were performed using MacCormack method and Baldwin-Lomax turbulence model to obtain global quantities of engineering interest rather than details of the flow field. Baldwin-Lomax model is calibrated for the flow over a flat plate on which the inner and outer region structures are reasonable. The transverse jet has a more complex turbulence structure with different length scales in the near-wall regions and over the jet's counter rotating vortices. The two-equation models are more appropriate for this flow field because the variations in scales at different regions are obtained directly when the equations for turbulence kinetic energy and a second quantity (ε or ω) are solved. Apart from using better turbulence models, comparisons of interior flow fields with experiments are needed to asses the prediction. Lee and Mitani[17] have studied the comparative performance of three transverse injectors for mixing augmentation in scramjet combustor using a three-dimensional Navier Stokes equation alongwith k-ω shear stress transport (SST) model. Edwards low diffusion flux splitting upwind difference scheme was used for discretisation. It has been observed that the mixing characteristics are strongly related to jet to cross flow momentum ratio. In case of higher values of momentum ratio, slower mixing rates, higher penetration, and more losses of stagnation pressure are observed. Sriram and Mathews[18] simulated transverse sonic injection in supersonic flow using Roe's approximate Riemann solver and k-ω turbulence model and captured detailed structures

of the Mach disc and other flow features. Quantitative agreement with the experimental results is very good in the upstream regions and close to the jet; while small differences appear in the downstream portion as the jet develops.

Numerical simulation of sonic transverse injection in supersonic flow in confined environment has not been reported adequately in the literature. Experimental condition of staged sonic injection behind a backward-facing step in rectangular duct has been explored numerically by Chakraborty[19], *et al*. using a Cartesian-based three-dimensional Navier Stokes solver alongwith *k*-ε turbulence model and obtained reasonable agreement with the experimental value of injectant penetration and various flow profiles at various axial locations of the combustor. The same experimental conditions were simulated by Manna and Chakraborty[20,21] with a 3D Reynolds Averaged Navier Stokes (RANS) solver alongwith *k*-ε turbulence model using a commercial solver and obtained very good comparisons of injectant penetration and spreading with the experimental results. Although, predicted flow profiles at various axial locations match with the experimental results, the values differ in the near-field region. Reliable predictions of detailed flow field allow better assessment of new ideas, for example, improved spreading and penetration of fuel in scramjet engine. For this, not only the global parameters need to be computed with good accuracy, also the computed local structures of the flow field must be accurate.

The study aims to demonstrate the capabilty of an indigenous 3D RANS code in simulating complex flow physics. Experimental condition of McDaniel[9,10], *et al*. was simulated numerically using an indigenously developed three-dimensional Navier stokes solver[22] based on Roe's approximate Riemann solver and k-ω turbulence model. The computed flow profiles at various axial locations have been compared with the experimental results and other numerical calculations.

2. EXPERIMENTAL SET-UP FOR THE COMPUTATIONS

The test cases for which numerical solutions have been presented here were taken from the experimental study of McDaniel[10], *et al*. Experiments were conducted to study the cold flow mixing of staged transverse sonic injection into Mach 2 flow behind a backward-facing step. Detailed measurements of various flow parameter profiles at various axial locations of the combustor were carried out using laser-induced iodine fluorescence (LIIF) and planar laser-induced iodine fluorescence (PLIIF) techniques. The schematic of the experimental set up for which the computations were carried out is presented in Fig. 2.

Details of the combustor geometry are presented in Table 1. The test section length (*L*), height (*H*), width (*W*) of the combustor is 71.85 mm, 21.29 mm, and 30.48 mm respectively. Two injectors, identical in size with diameter 1.93 mm, were placed at 12.7 mm and 25.4 mm from the step. The main purpose of the step is to isolate the inlet boundary layer from the pressure rise generated in the combustor. The step and the fuel injector staging are also expected to improve the penetration and mixing of fuel with the oxidiser and to create a recirculation region, which are important to sustaining the combustion.

The inflow parameters of the free-stream and sonic jet used in the simulations are summarized in Table 2. Free-stream Mach 2 air is having static pressure and temperature of 35 kPa and 167 K, respectively and iodine-seeded air stream with static pressure and temperature of 139 kPa and 250 K was used as the transverse jet.

3. NUMERICAL METHOD

The turbulent compressible flow can be described by Favre-averaged equations for conservation of mass, momentum, energy along with turbulent closure. The set of equations alongwith k-ω turbulence model can be written in the vector form as

$$\frac{\partial U}{\partial t}+\frac{\partial F}{\partial x}+\frac{\partial G}{\partial y}+\frac{\partial H}{\partial z}=S \qquad (1)$$

where $U = [\rho, \rho u, \rho v, \rho w, \rho E\ \rho k, \rho w]^T$ is a vector field of the state variable and *F, G* and *H* are flux vector consisting of viscous and inviscid fluxes, and *S* is a source vector. Here ρ is density, and *u, v* and *w* are components

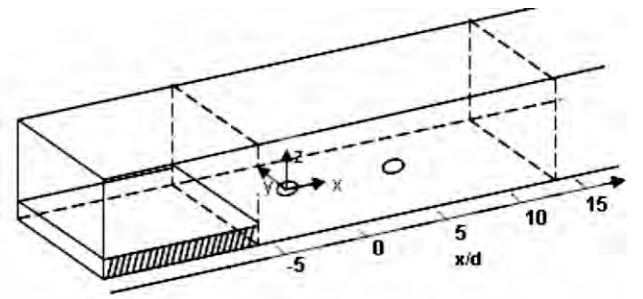

Figure 2. Schematic Representation of experimental setup of Mcdaniel[9,10], *et al.* for which computations were done.

Table1. Geometrical details of the combustor

Geometrical parameters	Values (mm)
Test Section length (*L*)	71.85
Test section height (*H*)	21.290
Test section width (*W*)	30.48
Step height (*h*)	3.218
Injector diameter (*D*)	1.93
Distance of step location from first injector	- 9.534
1st injector location (*x*)	0.0
2nd injector location (*x*)	12.7

Table 2. Inflow parameters for the computation

Parameter	Air stream	Injector
Free-stream static pressure, kPa (P_α)	35.0	139.0
Mach no (M)	2.0	1.0
Free-stream static temperature, K (T_α)	167.0	250.0
Free-stream velocity, m/s (u_α)	518.0	317.2
Molecular weight	28.8	28.86
Specific heat ratio (γ)	1.4	1.4

of velocity in *x, y* and *z* directions, respectively. The total energy *E* is sum of internal energy ($e = c_v T$), kinetic energy ($0.5(u^2 + v^2 + w^2)$) and turbulence kinetic energy *k*. The w represents the inverse of turbulent time scale, also related as specific turbulence dissipation with respect to the turbulence kinetic energy[23,24]. Wilcox's *k*-ω model with compressibility correction[24] was used in the present simulation. The transport equations of *k* and w are given by,

Turbulent kinetic energy (*k*) equation:

$$\frac{\partial}{\partial t}(\rho k) + \frac{\partial}{\partial x_i}(\rho k u_i) = \frac{\partial}{\partial x_j}\left(\Gamma_k \frac{\partial k}{\partial x_j}\right) + S_k$$

Specific dissipation rate (ω) equation:

$$\frac{\partial}{\partial t}(\rho \omega) + \frac{\partial}{\partial x_i}(\rho \omega u_i) = \frac{\partial}{\partial x_j}\left(\Gamma_\omega \frac{\partial \omega}{\partial x_j}\right) + S_\omega$$

The source terms S_k S_w of the k and w equations are given as

$$S_k = \left[\rho \frac{k}{\omega} - \frac{2}{3}\rho k \Sigma - \beta^* \rho k \omega\right] \quad \text{and}$$

$$S_\omega = \left[\alpha \frac{\omega}{k}\left(\Phi \rho \frac{k}{\omega} - \frac{2}{3}\rho k \Sigma\right) - \beta \rho \omega^2\right]$$

The source terms contain the strain invariant

$$\Phi = \left(\frac{4}{3}\frac{\partial u}{\partial x} - \frac{2}{3}\frac{\partial v}{\partial y}\right)\frac{\partial u}{\partial x} + \left(\frac{\partial u}{\partial y} + \frac{\partial v}{\partial x}\right)^2 + \left(\frac{4}{3}\frac{\partial u}{\partial x} - \frac{2}{3}\frac{\partial v}{\partial y}\right)\frac{\partial v}{\partial y},$$

and the divergence of the velocity field

$$\Sigma = \frac{\partial u}{\partial x} + \frac{\partial v}{\partial y}$$

Turbulence closure coefficients are

$\beta = 3/40$, $\beta^* = 9/100$, $\alpha = 5/9$, $\alpha^* = 1$, $\sigma = 1/2$, $\sigma^* = 1/2$

The equation of state $p = \rho RT$ was used to obtain the pressure from density and temperature. In the turbulence closure approach, the effective viscosity (μ_{eff}) becomes sum of the molecular viscosity (μ_m) and turbulent viscosity ($\mu_t = \rho k/\omega$), and the thermal conductivity becomes sum of molecular and turbulent parts using constant Prandtl numbers $Pr_m = 0.7$ and $Pr_t = 0.9$, respectively.

Time integration of the governing Eqn [1] was carried out using multistage Runge-Kutta (R-K) method to have second order accurate in time. The Eqn [1] was cast in the residual form as $\partial U/\partial t = R(u)$, and the numerical solution from n^{th} time step to $(n+1)^{th}$ time step was to be obtained from the following multistage operations:

$U^{(n)} = U^{(o)}$

$U^{(k)} = U^{(k-1)} + a_k R(U^{(k-1)})$ $(k = 1,..,m)$

$U^{(n+1)} = U^{(m)}$

For six stage ($m = 6$) operation, the $\alpha_1 = 0.0742$, $\alpha_2 = 0.1393$, $\alpha_3 = 0.02198$, $\alpha_4 = 0.3302$, $\alpha_5 = 0.5281$, $\alpha_6 = 1.0$.

While evaluating $R(U)$, one needs all the information about inviscid fluxes, viscous flues and the source term. Some special treatments are needed to suppress spurious oscillations near the shocks. Though central differencing (Jameson Scheme or MacComack method) with user tuned artificial diffusion was used in the past, use of upwind methods to evaluate inviscid fluxes are quite attractive, where the spurious oscillation near the shock can be reduced with the help of limiters. Though various upwind schemes were developed in the recent part, the flux difference splitting scheme developed by Roe[25] is quite popular. This Roe's approximate Riemann solver provides the inviscid interface flux as

$$F_{i+\frac{1}{2}} = \frac{1}{2}\left(F_L + F_R\right) - \frac{1}{2}\sum_{i=1}^{m} |\lambda_i| \Delta v_i \hat{R}^{(i)}$$

where *L* and *R* correspond to the left and right states respectively, $\hat{R}$ is matrix of right Eigen vectors the Δv becomes wave strength. The higher-order accuracy is obtained with monotone upstream-centered scheme for conservation laws (MUSCL), and the spurious oscillations were suppressed with min-mod limiter. The derivative terms in viscous and source terms are evaluated with central differencing formula.

The general boundary conditions for supersonic flow were used, where all the variables are fixed at the inflow, and all the variables are extrapolated at the exit. No slip and adiabatic conditions are imposed in the walls. Turbulent kinetic energy (*k*) is assumed zero at the wall and hydrodynamic smooth wall assumption is used to obtain the value of ω. At the inflow, *k* was specified by taking turbulence level of 5%, and ω was obtained by taking eddy viscosity to be equal to molecular viscosity. A log normalized residue of 10^{-4} is taken as the convergence. The code was validated systematically by simulating two-dimensional and three-dimensional transverse injections through slots[18,26,27] and comparing the experimental and numerical results.

4. RESULTS AND DISCUSSION

Three-dimensional computational domain was constructed from two rectangular blocks. The centre of the first hole was treated as origin for the coordinate system and the *x, y, z* coordinates are taken along the length, width and height of the combustor. A 110 x 30 x 45 non uniform structured grids were employed in the simulation. The grids were very fine near the wall and near the injection plane and relatively coarse in the other zones. Grid distribution was chosen from the grid-independence studies and was fine enough to resolve all essential features of the flow field. Schematic grid structure in the x-z plane is shown in Fig. 3. For the sake of clarity, only few grid points are shown in the vicinity of the lower wall. Actual grid contains very fine grid near the lower wall to capture complex recirculating flow and the jet structure. Grids are relatively coarse near the upper wall and no attempts were made to resolve the upper boundary layer in the duct.

Two sets of calculations were carried out for with and without transverse injection and qualitative behaviour of the flow has been analysed and the quantitative comparisons

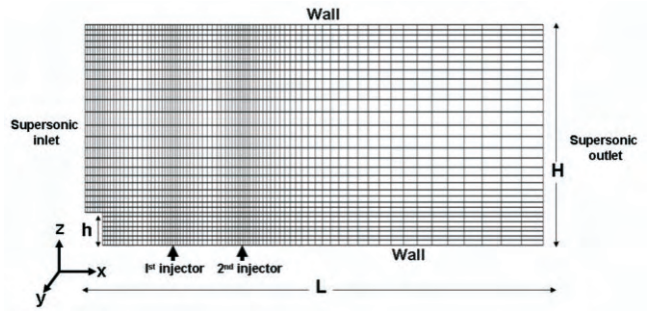

Figure 3. Grid distribution in the x-z plane in the computational domain.

has been made for various flow profiles at different axial stations by comparing with experimental results[10] and other numerical calculations[20, 21].

4.1 Flow Field Without Injection Case

Mach number distribution in the x-z plane and zoomed view of streamline pattern near the step is shown in Figs 4 and 5, respectively. The expansion waves from the step shoulder and compression waves after the shear layer attachment in the wall are clearly visible in the figures. Recirculation bubble downstream of the step is captured crisply in the simulation. The length of the recirculation bubble is about 5 D. The non-dimensionalised pressure profiles at combustor mid-plane have been compared with experimental results[10] and the computational results of Manna and Chakraborty[21] in Fig. 6 for different axial stations x/D = –2.05, 0, and 6.05. The pressure has been non-dimensionalised with free-stream static pressure while the distance along the height of the combustor is non-dimensionalised with the injector diameter. At x/D = –2.05, the lower wall pressure is at minimum and it increases as we proceed downstream. The constant pressure near the wall is indicating the height of the recirculation zone (z/D) which is about 1 at the first axial station and the height is reducing as one proceeds downstream. At x/D = 6.05, the free-stream pressure has almost recovered, indicating the end of the recirculation zone. For $z/D > 2$, the present computation agrees very well with the experimental result

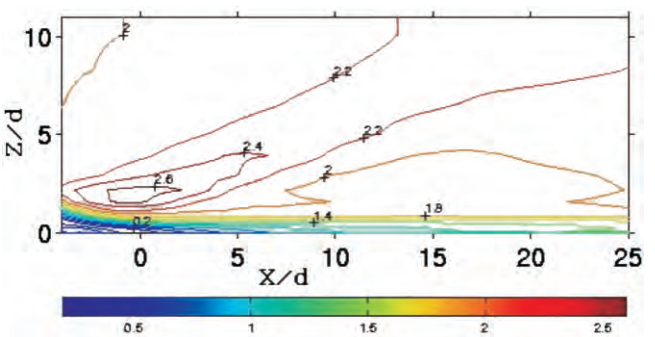

Figure 4. Mach number distribution in the x-z plane for no-injection case.

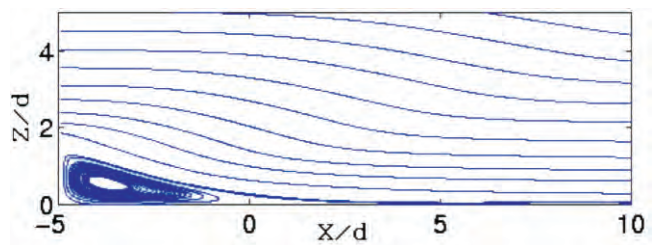

Figure 5. Zoomed view of streamline in the x-z plane near the step for no-injection case.

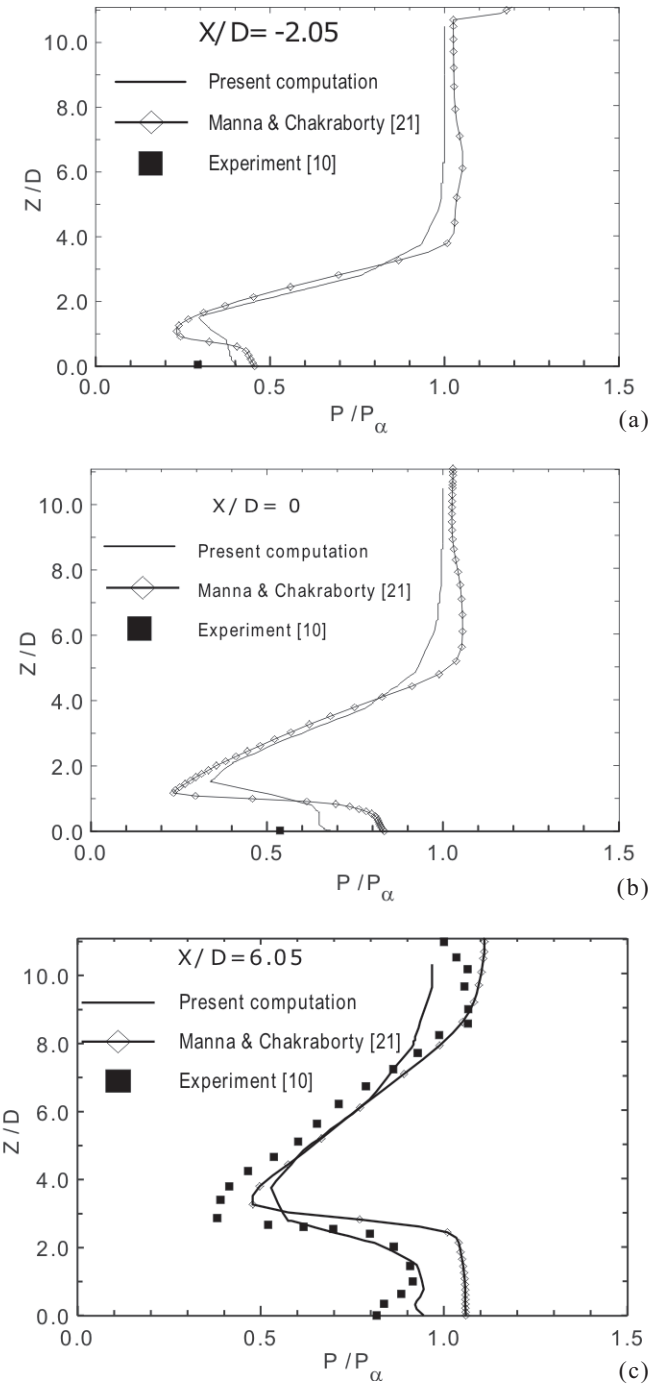

Figure 6. Comparison of pressure profiles at combustor mid plane at different axial stations x/D=-2.05, (b) x/D=0 (c) x/D = 6.05.

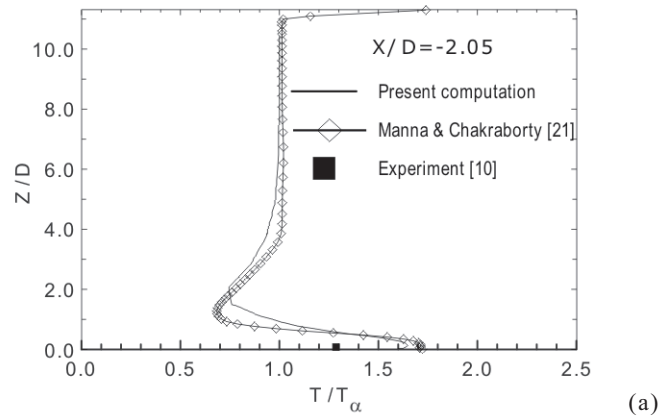

(a)

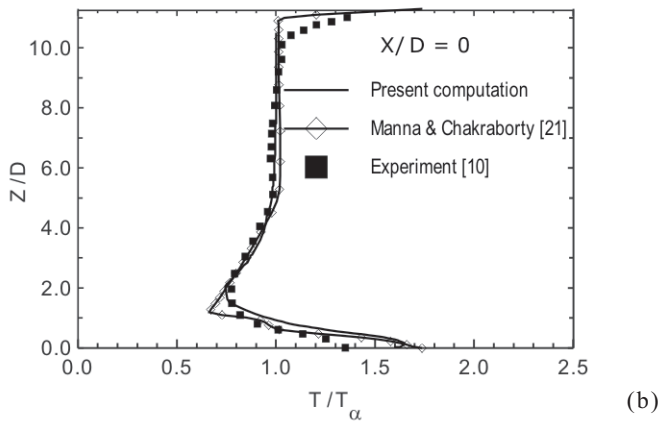

(b)

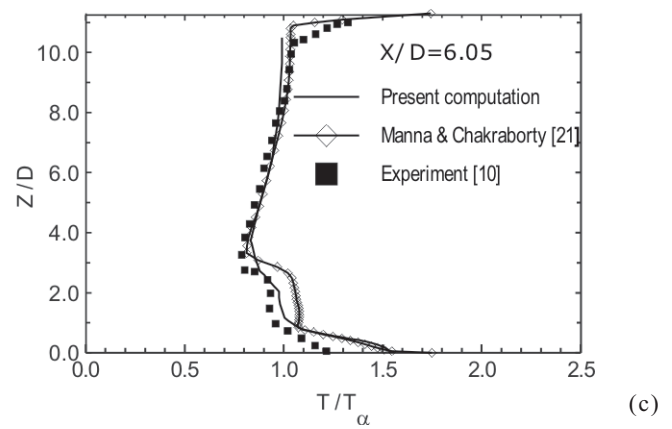

(c)

Figure 7. Comparison of temperature profiles at combustor mid plane at different axial stations (a) *x*/*D*=-2.05, (b) *x*/*D*=0 (c) *x*/*D* = 6.05.

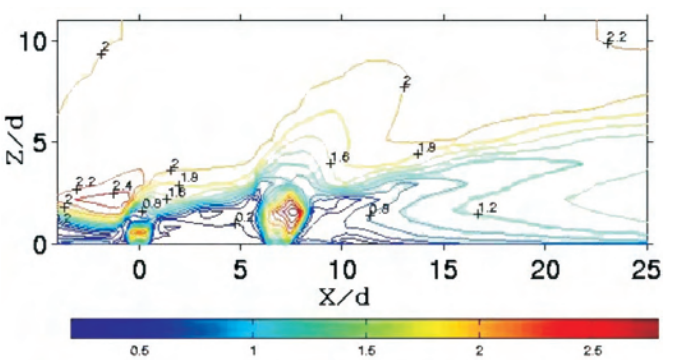

Figure 8. Mach number distribution at the injection plane.

at all the axial stations. Near-wall behaviour of the pressure has been captured better in the present computation compared to the computations of Manna and Chakraborty[21] with *k*-ε turbulence model which over predict the pressure values adjacent to the wall. The static temperature profile comparison with experimental values for three axial stations is presented in Fig. 7. The higher temperature near the wall is due to the boundary layer heating. The computed temperature profiles agree very well with the experimental values for all the three locations. The radial temperature profile of Manna and Chakraborty[21] slightly underpredicts the temperature near $z/D = 2$ for the first two axial points (x/D = -2.05 and 0), whereas it slightly overpredicts the temperature for the axial station $x/D = 6.05$.

4.2 Computation with Two Sonic Transverse Injections

The software was applied to simulate the staged sonic transverse injection into supersonic flow behind the backward-facing step. Longitudinal distribution of the Mach number in the injection plane is shown in Fig. 8. All the finer features of the flow field including the expansion from the step shoulder, the barrel shocks and the Mach discs from the injection points have been nicely captured in the simulation. The barrel shock and Mach disc for the first injection point was nearer to the wall compared to the second injection point although both the jets were injected with the same pressure. Jet from the second injection had penetrated more in the free-stream. Loss of total pressure of free-stream though the barrel shock of first injection point had made different momentum ratios for the two jets. More momentum ratio (jet total pressure/free-stream total pressure) of the second jet caused more penetration into the free-stream. The second jet showed dominant barrel shock structure and it was slightly lilted. The sub sonic portion behind the Mach disc is also seen in the figure. It is observed that accurate prediction of expansion of the jet from the lip of the injector is important for overall prediction

The computed non-dimensionalised pressure profiles at the injection plane along the height of the combustor has been compared with the experimental and other numerical results at three different axial station $x/D = 0$, 6.6, and 12.6 in Figs. 9(a)-9(c). The axial stations corresponding to $x/D = 0$ and 6.6 correspond to the injection point and pass through complex flow field of barrel shock, Mach disc was associated with transverse injection into the supersonic flow. The station at x/D=12.8 in the far downstream location. The flow expanded from injection pressure (~ 4 p_∞) to a low value of 0.5 p_∞. The pressure rise between $z/D = 1$ and 2 is due to the barrel shock. There is a good qualitative agreement between the experimental and computation results. In the region $z/D < 1.0$ and $z/D > 2.0$, there is very good quantitative agreement between the computation and experiment. In the region $1.0 < z/D < 2.0$, the computed pressure overpredicts the experimental value. In the zone, the different experiment results (PLIIF & LIIF)[10] show a difference of more than 30 per cent indicating a complex flow pattern. Numerical computations of Manna and

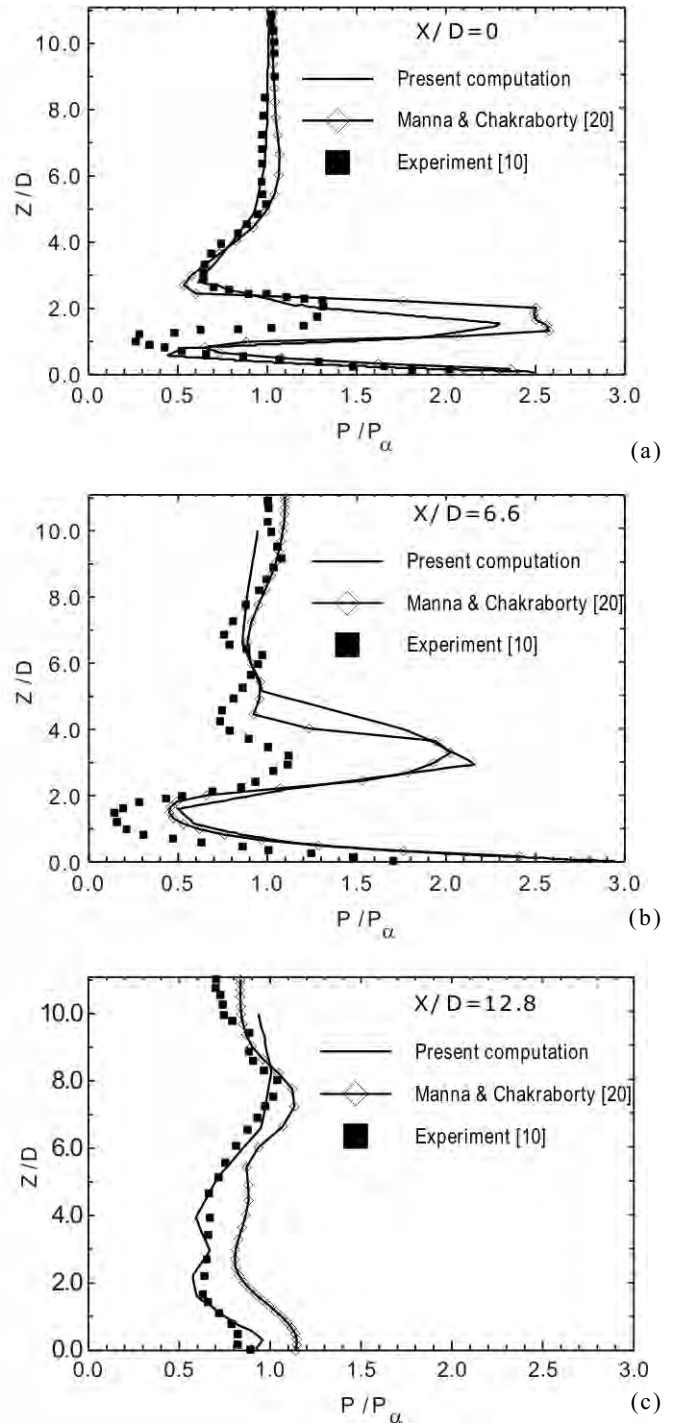

Figure 9. Comparison of pressure profiles at the injection plane at different axial stations (a) *x*/*D*=0, (b) *x*/*D*=6.6 (c) *x*/*D* = 12.8.

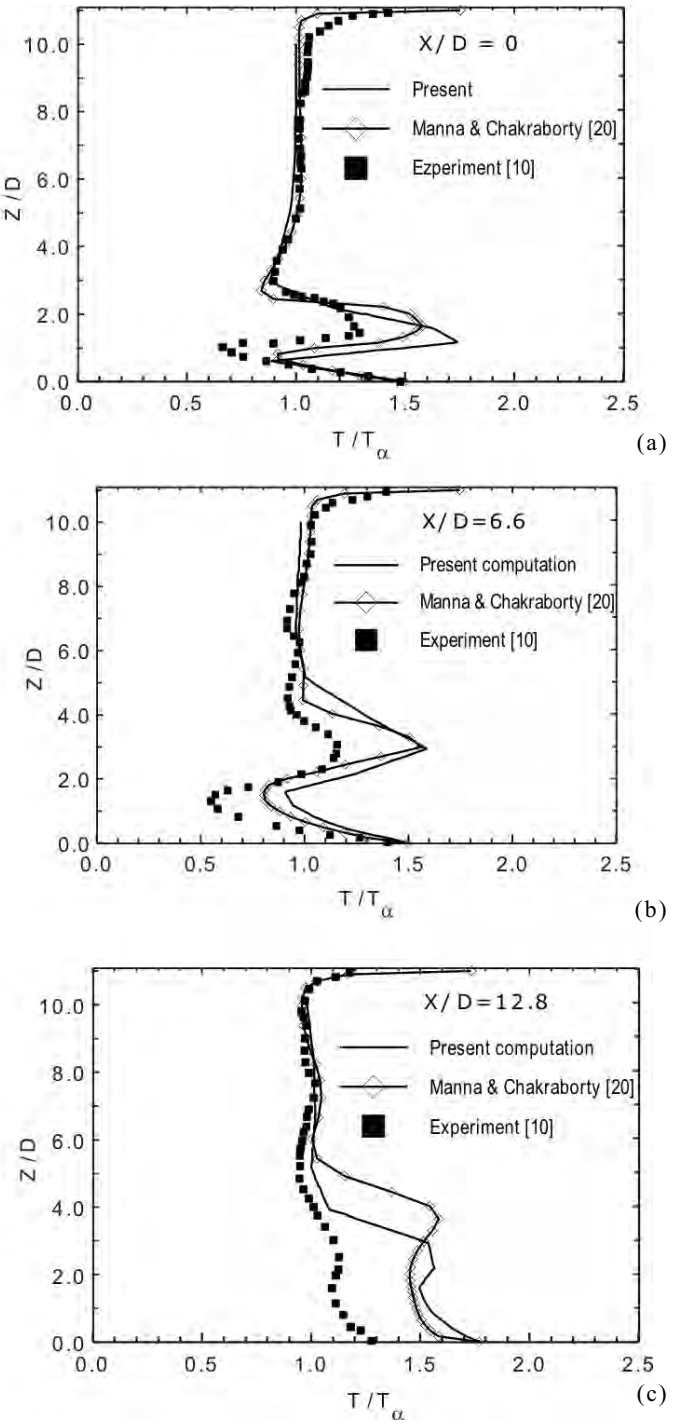

Figure 10. Comparison of temperature profiles at the injection plane at different axial stations (a) *x*/*D*=0, (b) *x*/*D*=6.6 (c) *x*/*D* = 12.8.

Chakraborty[20] with *k*-ε turbulence model overpredict the barrel shock pressure rise more than the present computation. Flow features for the second injection point of *x/D* = 6.58 show similar trend. The barrel shock height for the case is 2-D compared to less than 1-D for the first injection point. In the downstream wake region at *x/D*=12.8, the flow was more uniform and the present computation predict the experimental result very accurately. By comparing the flow profiles at various axial stations, it can be concluded that the performance of *k*-ω turbulence model is better than that of *k*-ε model.

The computed temperature profile at *x/D* = 0, 6.5, and 12.8 was compared with the experimental values and other numerical results in Figs. 10(a)-10(c). The temperature profiles are qualitatively similar with pressure profiles. The jet temperature was about 1.5 times more than the free-stream

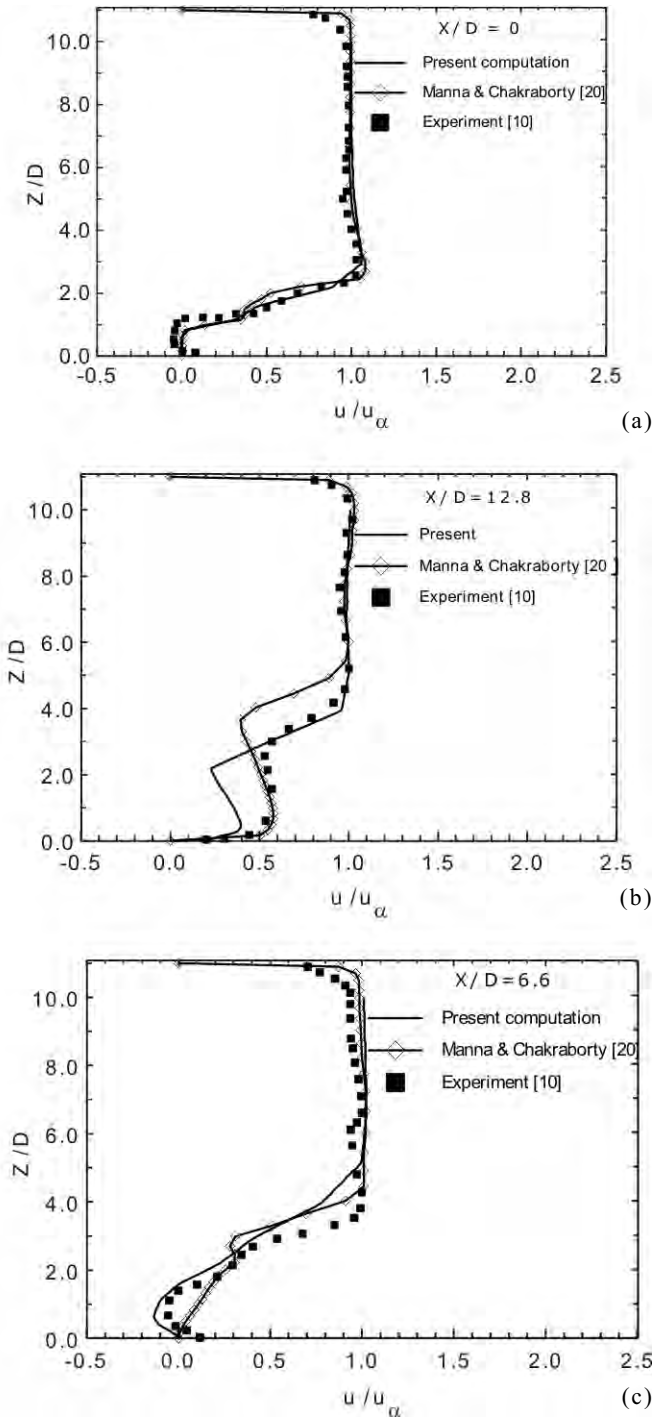

Figure 11. Comparison of streamwise velocity profiles at the injection plane at different axial stations (a) x/D = 0, (b) x/D = 6.6 (c) x/D = 12.8

temperature. The temperature decreases through expansion and increases through the barrel shock and finally get adjusted to the free-stream value. Like pressure profile, computed temperature profiles also overpredict the experimental values in the region $1 < z/D < 2$. In the other region, very good qualitative agreement between the computations and experimental values was obtained. At x/D = 6.6, similar trend is observed. In downstream wake location (x/D=12.8), both the present computation and computation of Manna and Chakraborty[20] overpredicts the experimental value up to z/D = 4. The present computation recovers the free-stream value at z/D = 4, whereas computation of Manna and Chakraborty[20] show a higher value for free-stream temperature recovery. The streamwise velocity profiles at the three locations are presented in Figs 11(a)-11(c). A good match with experimental and numerical results[20] is obtained for the velocity profile for all the three axial stations.Velocity profiles are showing a very complex flow pattern with number of inflexion points. In the first two axial stations, present computation predicts the experimental behaviour very clearly, whereas in the last axial station, up to $3 < z/D < 4$, predicted velocity was lower compared to the experimental value.

5. CONCLUSION

Transverse sonic injection into supersonic flow behind a backward-facing step in a three-dimensional rectangular duct has been explored numerically using an indigenous 3D RANS solver with Roe's scheme alongwith k-ω turbulence model with compressibility corrections. Multistage Runge–Kutta method was employed to have second order accuracy in time. All the finer details of flow structures including recirculation bubble behind a backward-facing step, barrel shocks, and Mach discs caused due to transverse injection and reattachment of shear layer in the downstream wake region have been captured crisply in the simulation. It has been observed that accurate prediction of expansion of the jet from the lip of the injector is important for overall prediction. Second jet was seen to penetrate more as the free-stream undergoes total pressure loss through the first injection barrel shock and increase the momentum ratio of the second jet to the free-stream. Computed profiles of various flow parameters at different axial locations in the duct match extremely well with the experimental results and the results of other numerical computations. In the near-wall and far-field regions, there is very good quantitative agreement between the computation and experiment. In the region of Mach disc and barrel shock, the computed pressure overpredicts the experimental value. The results demonstrate the robustness and accuracy of an indigenous RANS solver in predicting complex engineering flows.

ACKNOWLEDGMENT

The authors would like to thank Dr P Manna, Scientist DRDL for many fruitful discussions. He readily provided results of his computations for comparison. His help in preparing the manuscript of the paper is gratefully acknowledged.

REFERENCES

1. Gutmark, E.; Wilson, K.J.; Schadow, K.C.; Parr, T.P. & Hanson-Parr, D.M. Combustion enhancement in supersonic co-axial flow, AIAA Paper 89-2788, 1989.
2. Yu, K.; Wilson, K.J. & Schadow, K.C. On the use of combustor wall cavities for mixing enhancement. *In* the 3rd American Society of Mechanical Engineers,

Paper 99-7255, 1999.
3. Zukoski, E. E. & Spaid, F. W. Secondary injection of gases into a supersonic flow. *AIAA Journal*, 1964, **2**(10), 1689-696.
4. Schetz, J. A.; Hawkins, P. F. & Lehman, H. Structure of highly underexpanded transverse jets in a supersonic stream. *AIAA Journal*, 1967, **5**(5), 882-84.
5. Papamoschou, D., Hubbard, D. G. & Lin, M. Observations of supersonic transverse jets. AIAA paper 91-1723, 1991.
6. Yamauchi, K.; Kitadani, H.; Masuya, G.; Tomioka, S. & Izumikawa, M. Penetration of jets injected behind backward-facing step in supersonic stream. AIAA paper 99-2106, 1999.
7. Kuratani, N.; Ikeda, Y.; Nakajima, T.; Tomioka, S. & Mitani, T. Mixing characteristics of normal injection into a supersonic backward-facing step flow measured with PIV. AIAA paper 2002-0237, 2002.
8. Ikeda, Y.; Kuratani, N.; Nakajima, T.; Tomioka, S. & Mitani, T**.** M2.5 supersonic PIV measurement in step-back flow with the normal injection. AIAA paper 2002-0232.
9. McDaniel, J. C. & Graves, Jr. J. Laser-induced-fluorescence visualization of transverse gaseous injection in a nonreacting supersonic combustor. *J. Prop. Power*, 1988, **4**(6), 591-97.
10. McDaniel, J. C.; Fletcher, D. G.; Hartfield R. J. & Hollo, S. D. Staged transverse injection into Mach 2 flow behind a rearward facing step: A 3-D compressible test case for hypersonic combustor CFD validation. AIAA paper 91-5071, 1991.
11. Abbitt III, J. D.; Hartfield, R. J. & McDaniel, J. C. Mole-fraction imaging of transverse injection in a ducted supersonic flow. *AIAA Journal*, 1991, 29(3), 431-35.
12. Weinder, E. H., & Drummond J. P. Numerical study of staged fuel injection for supersonic combustion. *AIAA Journal*, 1982, **20(**10), 1426-431.
13. Rizzeta, D. P. Numerical investigation of slot jet injection into a turbulent supersonic stream. AIAA paper, 92-0839, 1992.
14. Clark, S.W. & Chan, S.C. Numerical investigation of a transverse jet for supersonic aerodynamic control. AIAA paper 92-0639, 1992.
15. Uenishi, K., Rogers, R.C. & Northam G.B. Numerical predictions of a rearward-facing-step flow in a supersonic combustor. *J. Prop. Power*, 1989, 5(2), 158-164.
16. Segal, C.; Haj-Hariri, H. & McDaniel, J. C. A numerical investigation of hydrogen combustion in Mach 2 airflow. AIAA Paper 92-0341, 1992.
17. Lee, S. H. & Mitani, T. Mixing augmentation of transverse injection in scramjet combustor. *J. Prop. Power*, 2003, **19**(1), 115-24.
18. Sriram, A.T. & Mathew, Joseph. Numerical simulation of transverse injection of circular jets into turbulent supersonic streams. *J. Prop. Power*, 2008, **24**(1), 45-54.
19. Chakraborty, Debasis; Roychowdhury, A. P.; Ashok V. & Pradeep Kumar, Numerical investigation of staged transverse sonic injection in Mach 2 stream in confined environment. *Aeronautical Journal*, 2003, **107**(1078), 719-29.
20. P. Manna & Chakraborty, Debasis. Numerical investigation of transverse sonic injection in a nonreacting supersonic combustor. *ASME J. Aero. Engg. Part G*, **219**(3), 205-15.
21. P. Manna & Chakraborty, Debasis. Numerical investigation of confinement effect on supersonic turbulent flow past backward-facing step with and without transverse injection. *J. Aero. Sci. Technolo.*, 2009, **61**(2), 283-94.
22. Sriram, A.T. Numerical simulations of transverse injection of plane and circular sonic jets into turbulent supersonic cross flows. Department of Aerospace Engineering, Indian Institute of Science, Bangalore, India, 2003. Ph.D. Thesis.
23. Anderson, D.A.; Tannehill, J.C. & Pletcher, R.H. Computational fluid mechanics and heat transfer. Hemisphere, Washington, D.C., 1984.
24. Wilcox, D.C. Turbulence modeling for CFD. DCW Industries, Inc., La Cañada, CA, 1993.
25. Roe, P.L. Characteristic based schemes for the Euler equations. *Ann. Rev. Fluid Mech.*, 1986, **18**, 337-65.
26. Sriram, A.T. & Mathew, J. Numerical simulation of sonic jet injected into a supersonic crossflow with k-ω turbulence model. *J. Aero. Sci. Technol*., 2003, **55**(3).
27. Sriram, A.T. & Mathew, J. Improved prediction of plane transverse jets in supersonic crossflows. *AIAA Journal*, 2006, **44**(2), 405-08.

Contributors

Dr A.T. Sriram obtained his PhD in Aerospace Engineering, from Indian Institute of Science, Bengaluru. His specialisation is on computations of compressible turbulent flows applicable to turbomachines and propulsion systems (SCRAMJET Engines). His post doctoral work includes research at CGPL (IISc, Bangalore), DRDL (Hyderabad) and University of Virginia. His research interest includes interaction of shock wave with free-stream turbulence and turbulent boundary layers, non-reacting and reacting supersonic shear layers and flame-acoustic interactions.

Dr Debasis Chakraborty obtained his PhD in Aerospace Engineering from Indian Institute of Science, Bengaluru. Presently, he is working as Technology Director, Computational Dynamics Directorate, DRDL, Hyderabad. His research interests are CFD, aerodynamics, high-speed combustion, and propulsion. He has about 30 journal and 40 conference publications.